6-25-2019

Equilibrium in the Catalytic Condensation of Carboxylic Acids with Methyl Ketones to 1,3-Diketones and the Origin of the Reketonization Effect

Alexey Ignatchenko
St. John Fisher University, aignatchenko@sjfc.edu

Thomas DiProspero
St. John Fisher University, tjd01678@students.sjf.edu

Heni Patel
St. John Fisher University, hp03692@students.sjf.edu

Joseph R. LaPenna
St. John Fisher University, jrl05799@students.sjf.edu

Publication Information

Ignatchenko, Alexey; DiProspero, Thomas; Patel, Heni; and LaPenna, Joseph R. (2019). "Equilibrium in the Catalytic Condensation of Carboxylic Acids with Methyl Ketones to 1,3-Diketones and the Origin of the Reketonization Effect." *ACS Omega* 4.6, 11032-11043.

Equilibrium in the Catalytic Condensation of Carboxylic Acids with Methyl Ketones to 1,3-Diketones and the Origin of the Reketonization Effect

Abstract

Acetone is the expected ketone product of an acetic acid decarboxylative ketonization reaction with metal oxide catalysts used in the industrial production of ketones and for biofuel upgrade. Decarboxylative cross-ketonization of a mixture of acetic and isobutyric acids yields highly valued unsymmetrical methyl isopropyl ketone (MIPK) along with two less valuable symmetrical ketones, acetone and diisopropyl ketone (DIPK). We describe a side reaction of isobutyric acid with acetone yielding the cross-ketone MIPK with monoclinic zirconia and anatase titania catalysts in the absence of acetic acid. We call it a reketonization reaction because acetone is deconstructed and used for the construction of MIPK. Isotopic labeling of the isobutyric acid's carboxyl group shows that it is the exclusive supplier of the carbonyl group of MIPK, while acetone provides only methyl group for MIPK construction. More branched ketones, MIPK or DIPK, are less reactive in their reketonization with carboxylic acids. The proposed mechanism of reketonization supported by density functional theory (DFT) computations starts with acetone enolization and proceeds via its condensation with surface isobutyrate to a β-diketone similar to β-keto acid formation in the decarboxylative ketonization of acids. Decomposition of unsymmetrical β-diketones with water (or methanol) by the retrocondensation reaction under the same conditions over metal oxides yields two pairs of ketones and acids (or esters in the case of methanol) and proceeds much faster compared to their formation. The major direction yields thermodynamically more stable products—more substituted ketones. DFT calculations predict even a larger fraction of the thermodynamically preferred pair of products. The difference is explained by some degree of a kinetic control in the opposite direction. Reketonization has lower reaction rates compared to regular ketonization. Still, a high extent of reketonization occurs unnoticeably during the decarboxylative ketonization of acetic acid as the result of the acetone reaction with acetic acid. This degenerate reaction is the major cause of the inhibition by acetone of its own rate of formation from acetic acid at high conversions.

Keywords

fsc2020

Disciplines

Chemistry

ACS OMEGA

Article

Cite This: ACS Omega 2019, 4, 11032−11043

http://pubs.acs.org/journal/acsodf

Equilibrium in the Catalytic Condensation of Carboxylic Acids with Methyl Ketones to 1,3-Diketones and the Origin of the Reketonization Effect

Alexey V. Ignatchenko,* Thomas J. DiProspero, Heni Patel, and Joseph R. LaPenna

Chemistry Department, St. John Fisher College, 3690 East Avenue, Rochester, New York 14618, United States

Supporting Information

ABSTRACT: Acetone is the expected ketone product of an acetic acid decarboxylative ketonization reaction with metal oxide catalysts used in the industrial production of ketones and for biofuel upgrade. Decarboxylative cross-ketonization of a mixture of acetic and isobutyric acids yields highly valued unsymmetrical methyl isopropyl ketone (MIPK) along with two less valuable symmetrical ketones, acetone and diisopropyl ketone (DIPK). We describe a side reaction of isobutyric acid with acetone yielding the cross-ketone MIPK with monoclinic zirconia and anatase titania catalysts in the absence of acetic acid. We call it a reketonization reaction because acetone is deconstructed and used for the construction of MIPK. Isotopic labeling of the isobutyric acid's carboxyl group shows that it is the exclusive supplier of the carbonyl group of MIPK, while acetone provides only methyl group for MIPK construction. More branched ketones, MIPK or DIPK, are less reactive in their reketonization with carboxylic acids. The proposed mechanism of reketonization supported by density functional theory (DFT) computations starts with acetone enolization and proceeds via its condensation with surface isobutyrate to a β-diketone similar to β-keto acid formation in the decarboxylative ketonization of acids. Decomposition of unsymmetrical β-diketones with water (or methanol) by the retrocondensation reaction under the same conditions over metal oxides yields two pairs of ketones and acids (or esters in the case of methanol) and proceeds much faster compared to their formation. The major direction yields thermodynamically more stable products—more substituted ketones. DFT calculations predict even a larger fraction of the thermodynamically preferred pair of products. The difference is explained by some degree of a kinetic control in the opposite direction. Reketonization has lower reaction rates compared to regular ketonization. Still, a high extent of reketonization occurs unnoticeably during the decarboxylative ketonization of acetic acid as the result of the acetone reaction with acetic acid. This degenerate reaction is the major cause of the inhibition by acetone of its own rate of formation from acetic acid at high conversions.

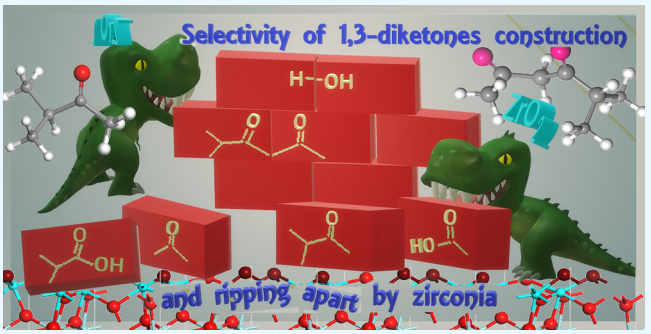

1. INTRODUCTION

Catalytic conversion of carboxylic acids into methyl ketones is an important industrial process for the preparation of fine chemicals and intermediates.[1−5] The first industrial scale production of acetone was already operating more than a century ago, before World War I, utilizing acetic acid derived from pyrolysis of wood.[6] In recent years, decarboxylative ketonization of carboxylic acids has been also viewed as a promising step for the development of biofuel technology, which has a purpose of reducing the amount of various carboxylic acids in otherwise chemically unstable pyrolysis oil.[7]

The mechanism for the catalytic formation of a ketone molecule from two molecules of a carboxylic acid involves a Claisen-like condensation between α-carbon of the enolized carboxylate and the carboxyl group of the second molecule followed by dehydration to the unstable β-keto carboxylate and its subsequent decarboxylation (Scheme 1). The use of acids rather than esters in the heterogeneous catalytic version of the Claisen condensation is made possible because of the trapping of carboxylic protons on the metal oxide surface.[8]

Despite being studied for over a century, catalytic decarboxylative ketonization is a more complicated reaction relative to how it has been described in the literature so far.[9−11] What has still to be understood is a considerable degree of side reactions going unnoticed and the fact that the major pathway is reversible. First, the reversibility of all of the steps of the reaction mechanism has been only recently proposed in the computational study on a zirconium oxide catalyst.[8] Subsequently, experimental evidence was found supporting the idea that the formation and decomposition of the β-keto acid intermediate in Scheme 1 are reversible. That is to say, ketones can enolize and condense with carbon dioxide back to β-keto acids—unstable intermediates.[12]

Received: April 25, 2019
Accepted: June 11, 2019
Published: June 25, 2019

DOI: 10.1021/acsomega.9b01188
ACS Omega 2019, 4, 11032−11043

Scheme 1. Mechanism of the Catalytic Decarboxylative Ketonization of Carboxylic Acids on Zirconia

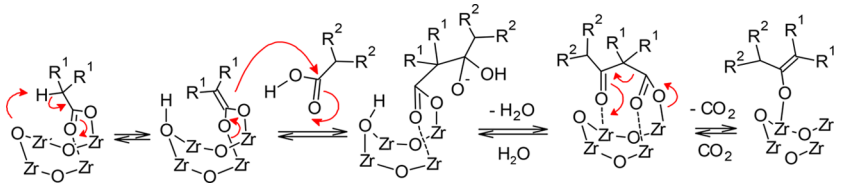

Scheme 2. Methyl Ketone Reketonization via Their Enolization and Claisen-like Condensation with Carboxylic Acids Followed by Retrocondensation to a Different Pair of Acid/Ketone

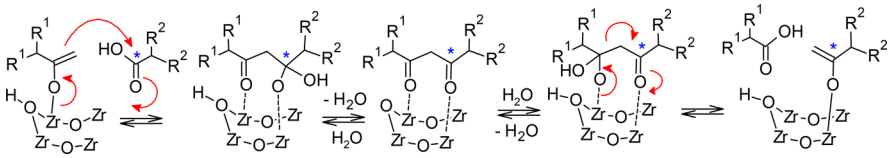

The present work extends the above chemistry by adding starting carboxylic acids to the list of electrophiles participating in the condensation with the enolized ketone products. We hope that the current study will draw attention to the kinetic consequences of many side reactions taking place during the catalytic decarboxylative ketonization of carboxylic acids on metal oxides.

Condensation between the enolized molecule of a ketone and a molecule of carboxylic acid catalyzed by metal oxides should lead to 1,3-diketones, called β-diketones, but it has not been well documented in the literature.[13] Similarly to the fate of β-keto acids, the reaction does not stop at the formation of the β-diketone on the surface of metal oxides because of the two competing retrocondensation reactions going in opposite directions (Scheme 2).

A similar behavior is known for a noncatalytic condensation in solutions between ketones and esters of trifluoroacetic acid when using a stoichiometric amount of NaH base. The initial condensation transforms an ester function to one of the two keto groups of the 1,3-diketone intermediate. Then, it is followed by a retrocondensation on the other keto group converting it to another ester and yielding trifluoromethyl ketones (Scheme 3).[14,15] The product mixture contains

Scheme 3. Preparation of Trifluoromethyl Ketones Similar to Reketonization

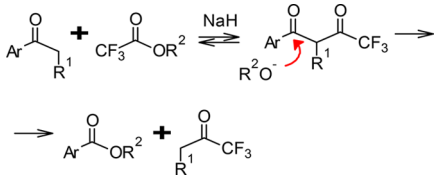

exclusively the ester of the aromatic acid and trifluoromethyl ketone without starting materials, which makes it a highly selective synthetic method.

In a separate experiment, when the intermediate β-diketone is treated by OH^- or CH_3O^-, it decomposes into two pairs of a ketone−acid (or a ketone−ester) via the retrocondensation reaction involving either one of the two keto groups.[15]

The equilibrium in Scheme 3 is shifted to the right, but in view of the results of the above decomposition, it is not because one of the carbonyl groups of the β-diketone is more susceptible to the nucleophilic attack. The observed selectivity is explained by a low nucleophilicity of the α-carbon on the enolate of the trifluoromethyl ketone, which slows down its conversion back to the diketone. Acylation of the trifluoromethyl-substituted enolate proceeds on oxygen rather than on carbon, and the reesterification of the O-acylated enol by R^2O^- under the reaction conditions brings back the trifluoromethyl ketone. Such asymmetry of the ketone reactivity is responsible for the selective formation of trifluoromethyl ketones.

In the current work, we describe the results of our study of a similar asymmetric effect for the catalytic version of the Claisen-like condensation on metal oxides between methyl ketones and carboxylic acids when two simple alkyl groups with a different degree of branching are used in place of −Ar and $-CF_3$. The resulting unsymmetrical β-diketone intermediate decomposes in the opposite direction and yields a coupled pair of an acid and a ketone, which is formally described as the methyl group transfer. We call it the reketonization reaction that occurs when an alkyl group of a ketone prepared from one carboxylic acid is replaced by an alkyl group from another carboxylic acid through a series of condensation and retrocondensation reactions.

Recognizing the reketonization reaction and understanding its mechanism will have a significant impact on the industrial technology of asymmetric ketone preparation and on the complete understanding of the mechanism and kinetics of the related reaction, the decarboxylative ketonization of carboxylic acids.

2. EXPERIMENTAL SECTION

2.1. Abbreviations. Catalysts are abbreviated as follows: ZR, untreated zirconia; ZK, KOH-treated zirconia; TK, KOH-treated titania.

Acids, ketones, and 1,3-diketones are numbered by letters according to the type and number of alkyl groups found in them: **A** for methyl, **B** for isopropyl, and **C** for ethyl (Chart 1).

2.2. Catalysts and Reagents. Monoclinic zirconium oxide and the anatase form of titanium oxide, in a shape of cylinders, 3−5 mm in length and 3 mm in diameter, were purchased from Alfa Aesar. Acetone (**AA**), 3-methylbutan-2-one (**AB**), MIPK, 2,4-dimethyl-3-pentanone (**BB**), DIPK, 2-butanone (**AC**) (MEK), acetylacetone (**AAA**), 3,3-dimethyl-2,4-pentanedione (**ABA**), acetic **A** and isobutyric **B** acids with natural isotopes, and isotopically labeled isobutyric acid, $(CH_3)_2CH^{13}CO_2H$, were purchased from Aldrich. 2,6-

DOI: 10.1021/acsomega.9b01188
ACS Omega 2019, 4, 11032−11043

Chart 1. Compounds Numbering

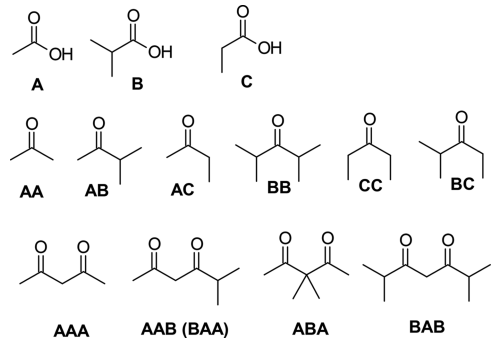

Dimethyl-3,5-heptanedione, **BAB**, was purchased from Acros Organics.

2.3. Preparation of 5-Methylhexane-2,4-dione (AAB). The synthesis and purification were based on a patented procedure.[16] Toluene (150 mL), ethyl acetate (36.2 g, 0.41 mol), and NaH (15.7 g, 0.39 mol; 60% oil dispersion) were placed in a 1 L three-necked flask and heated to 70 °C. 3-Methyl-2-butanone (20.1 g, 0.23 mol) was added dropwise over 1 h under stirring while maintaining the temperature at 70 °C. After addition was complete, the reaction mixture was stirred at 70° C for 1.5 h and chilled to room temperature. A portion of ethanol (5 mL) was added under stirring to decompose unreacted NaH. The precipitated solid was dissolved by adding 100 mL of water, and the reaction mixture was stirred overnight at ambient temperature to complete hydrolysis of esters at a pH value of 12.5. The top organic layer containing impurities of a low acidity was removed, and the remaining aqueous layer was extracted twice with 30 mL portions of hexane. The aqueous layer was acidified by carefully adding HCl (15%) to a pH value of 8.0. The organic layer was separated and saved. The aqueous layer was extracted twice with 30 mL portions of hexane. The combined organic phases were dried over CaSO4 and concentrated under vacuum in a rotary evaporator, and the residue was distilled. Fraction boiling at 81−85 °C/27 mm Hg (lit. bp 70−74 °C/20 mm Hg[17]), 13.8 g (46.1% yield), was collected and analyzed by GC. The GC-estimated purity of the product was 98.8%.

2.4. Catalyst Preparation and Characterization. KOH-treated catalysts were used from the same batches that were used in the previous study.[4] Pellets were crushed and sieved to obtain different fractions for the kinetic fit experiment in the continuous flow reactor. A fraction of 0.2−0.75 mm was used for all studies. Monoclinic zirconia had a median pore diameter of 160/600 Å, bimodal total pore volume of 0.30 mL/g, and BET surface area of 48 m^2/g for the untreated catalyst and 45 m^2/g for the KOH-treated catalyst determined by nitrogen adsorption at 77 K. Anatase titania had a median pore diameter of 270 Å, total pore volume of 0.29 mL/g, and BET surface area of 42 m^2/g for the KOH-treated catalyst.

2.5. Continuous Flow Reactor. A tubular reactor, 3.0 mm in internal diameter, 200 mm in length equipped with a thermocouple positioned in the center of the heated zone, was used as previously described.[4] The bottom and the top of the catalyst bed were each filled with PRO-PAK metal-packing chips. The catalyst was supported between two pieces of quartz wool. The diketone solution in methanol or water or a mixture of ketones and carboxylic acids at the specified molar ratios, feed rates, and temperatures (Tables S1−S3 in the Supporting Information) was continuously pumped by a New Era syringe pump, model NE-1000, through a preheating line, 1.6 mm in diameter, to the top of the reactor. All experiments were conducted at atmospheric pressure. Deionized water or methanol was pumped through the reactor between switching feeds. Liquid products were collected from the outlet of the condenser and analyzed by GC/MS.

Average turnover frequencies (TOF, s^{-1}) were calculated from the number of moles consumed or produced per second on a catalyst with a known weight and BET surface area assuming four Zr or Ti metal surface atoms in one catalytic site and average densities of 8.4 nm^{-2} on monoclinic zirconia[8,18] and 5.7 nm^{-2} on anatase titania[11,18] determined by DFT studies.

Residence times were calculated by dividing the volume of the catalyst bed by the volume of the ideal gas produced from vaporization of a known number of moles of all liquid components in the feed pumped per unit of time.

2.6. Identification of the Products. Products were analyzed by a Thermo Scientific TRACE 1300 gas chromatograph equipped with a Restek XTI-5 capillary column (30 m in length, 0.25 mm in diameter, 0.25 μm in phase thickness), an FID detector for quantitative analysis and with an HP-5 MS UI capillary column (30 m in length, 0.25 mm in diameter, 0.25 μm phase thickness), and a Thermo Scientific ISQ single quadrupole mass selective detector for identification analysis. Ketones **AA**, **AB**, and **BB** and acids and methyl esters of **A** and **B** were identified by matching GC retention times and MS spectra with authentic samples.

2.7. GC Quantitative Analysis Method. Helium carrier gas with a constant column flow (0.9 mL/min), a split mode of injection with a split ratio of 100:1, and an oven temperature of 50 °C holding for 5 min and then rising 15 °C/min were used for the quantitative analysis method. The amounts of all products and unreacted reagents were calculated using the integration of the corresponding peaks relative to the area of the internal standard added to the collected product samples, methyl *tert*-butyl ether (MTBE) for β-diketones decomposition, and methanol for the reaction of isobutyric acid with acetone. Preliminary calibration of carboxylic acids, methyl esters, and ketones included three levels of their concentration.

2.8. "Inside GC/MS" Pulse Microreactor. A GC/MS pulse microreactor was built and used as previously described.[18,19]

2.9. Multilevel Factorial Design of Experiments (DOE) Model. The DOE model for the isobutyric acid reaction with acetone included three experimental factors, temperature (°C), molar fraction of acid B (%), and liquid hourly space velocity (LHSV, h^{-1}), with three levels of each factor and two blocks. The amounts of ketone products, AB and BB, were measured, and their rates of formation (mmol/g-cat/h) were calculated and used as response variables in the regression analysis. The selected design included 16 runs, using the same portion of the catalyst for all 16 runs and collecting one product sample for each run (Table S1). Prior to DOE experiments, each catalyst was aged by running the reaction at 375−400 °C for at least 2 h. A quadratic model of the process factors with five coefficients was used (Table S2 in the Supporting Information). Insignificant process factors and their interactions were eliminated during regression analysis to achieve the p value less than 5%. R^2 values were ranged from 65% to 99%.

DOE models for β-diketone decomposition included two experimental factors, temperature (°C) and molar fraction of

DOI: 10.1021/acsomega.9b01188
ACS Omega 2019, 4, 11032−11043

β-diketone (%) with three levels of each factor and two blocks. The amounts of ketones and ester products were measured, and their rates of formation (TOF s^{-1}) were calculated and used as response variables in the regression analysis. The selected design had six runs, using the same catalyst loading for all six runs and collecting two product samples for each run (Table S4 in the Supporting Information). Regressions coefficients are shown in Table S5 of the Supporting Information.

2.10. Computational Method. Density functional theory (DFT) calculations for periodic structures were performed with the DMol[3] program from Dassault Systèmes Biovia Corp.[20] previously used in our study of the decarboxylative ketonization mechanism[8,21] and water interaction with zirconia and titania surfaces.[18] Graphical displays were generated with Materials Studio. Electron exchange and correlation were described by the generalized gradient approximation (GGA) based on the work of Perdew et al. using the PBE functional[22] with a Tkatchenko−Scheffler (TS) exchange correlation[23] to address intermolecular dispersive interactions.

Periodic slab geometry was used to model zirconia surfaces adopting previously used models.[8,18,21] A (111) surface was cleaved to a depth of ∼12 Å, and a vacuum slab of 20 Å in thickness was built above the surface. A supercell was constructed of 16 zirconium atoms and 32 oxygen atoms. The top three surface layers, consisting of twelve ZrO2 units, were allowed to relax, while the bottom layer of four ZrO2 units was constrained. Energy minimization and frequency calculations were performed for the obtained supercell with and without adsorbed molecules by density functional calculations using the double numerical plus polarization basis set. Core electron treatment included all electron relativistic options. All calculations were performed spin restricted. A real space cutoff of 4.6 Å and a k-point sampling spacing of 0.05 $Å^{-1}$ were used. SCF density convergence, optimization energy convergence, and gradient convergence were set to 1×10^{-5}, 2×10^{-5}, and 4×10^{-3} a.u., respectively. Molecule geometry in the gas phase was optimized, and frequencies were calculated using the same method. Thermodynamic quantities were computed from vibrational frequency calculations.

Transition states were found using the improved tangent algorithm for the nudged elastic band method,[24] and their geometry was subsequently refined, that is, each TS structure was optimized to its minimum according to all the coordinates (positive frequencies) and to its maximum with respect to the reaction coordinate (negative frequency). Frequency calculations were used to characterize each TS as a first-order saddle point with only one imaginary frequency.

3. RESULTS

3.1. Catalytic Condensation of Acetone with Isobutyric Acid. Mixtures of acetone and isobutyric acid in molar ratios from 1:9 to 9:1 were converted to a mixture of MIPK and DIPK within the temperature range from 250 to 450 °C in the hot tube reactor filled with anatase titania or zirconia catalysts. The amount of products was measured by GC/FID analysis and used to calculate reaction rates averaged over the conversion range. Data points in a set of 16 statistically designed experiments were used in the regression analysis to obtain average reaction rates as a continuous function of the temperature and molar fraction of isobutyric acid with three different catalysts for the formation of MIPK (Figure 1) and DIPK (Figure 2).

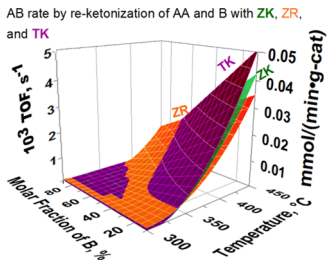

Figure 1. Dependence of the MIPK (**AB**) rate of formation on temperature and on the molar fraction of isobutyric acid (**B**) in the mixture with acetone (**AA**) for ZR, ZK, and TK catalysts at a residence time of 1.7 s and LHSV of 7 h^{-1}.

Traces of acetic acid were found in some of the experiments. Because of the small amount of acetic acid formed and only at some conditions, it was not included in the regression analysis. Conversion of acetic acid to acetone proceeds much faster under the same conditions and with the same catalysts[4] compared to its formation in the above reaction.

KOH-treated catalysts, ZK and TK, had slightly higher activity for the production of MIPK from acetone and isobutyric acid compared to the untreated catalyst, ZR. The highest activity for MIPK production was found with the TK catalyst. Surface charts (Figure 1) have a similar shape for all three catalysts. The MIPK rate with all three catalysts had a linear dependence on the fraction of isobutyric acid and a second degree polynomial dependence on temperature (Table S2 in the Supporting Information).

Formation of DIPK from two molecules of isobutyric acid was favored at high temperatures and at high molar fraction of isobutyric acid, while MIPK formation from acetone and isobutyric acid was favored at high molar fraction of acetone and started at lower temperatures (Figure 2). The selectivity to MIPK defined as the ratio of the MIPK rate to the sum of MIPK and DIPK rates was the highest with the TK catalyst among all studied catalysts under most conditions.

The above data demonstrated that acetone can be used instead of acetic acid to produce the cross-ketone, MIPK, in the reaction with isobutyric acid. Rates of MIPK formation have been also measured for the regular cross-ketonization reaction between acetic and isobutyric acids under the same conditions. When two methods are compared directly (Figure 3), it can be seen that rates of MIPK formation are faster for the isobutyric acid condensation with acetic acid rather than with acetone. The difference between the rates in two methods becomes smaller at higher temperature and at lower concentration of isobutyric acid.

3.2. Condensation of Branched Ketones with Carboxylic Acids. Attempts to produce a similar reketonization effect in the reaction of branched ketones, MIPK or DIPK, with acetic or isobutyric acids were less successful. In the attempted reaction of MIPK with acetic acid under the same conditions, only traces of isobutyric acid and DIPK were detected in addition to a large amount of acetone coming from the condensation between two molecules of acetic acid.

Theoretically, reketonization could proceed in two directions depending on the side of the MIPK molecule, **AB**, which is enolized. In one direction, enolization through the

DOI: 10.1021/acsomega.9b01188
ACS Omega 2019, 4, 11032−11043

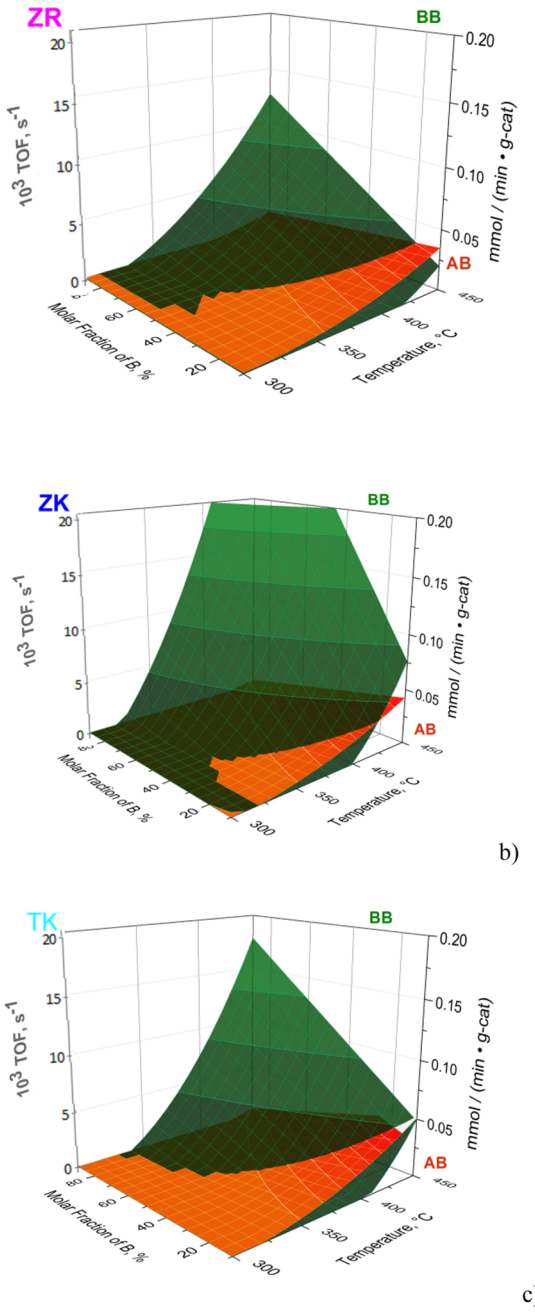

Figure 2. Comparison of the reaction rates for MIPK (**AB**) and DIPK (**BB**) formation with (a) Zr, (b) ZK, and (c) TK catalysts depending on temperature and molar fraction of isobutyric acid (**B**) in the mixture with acetone at a residence time of 1.7 s and LHSV of 7 h^{-1}.

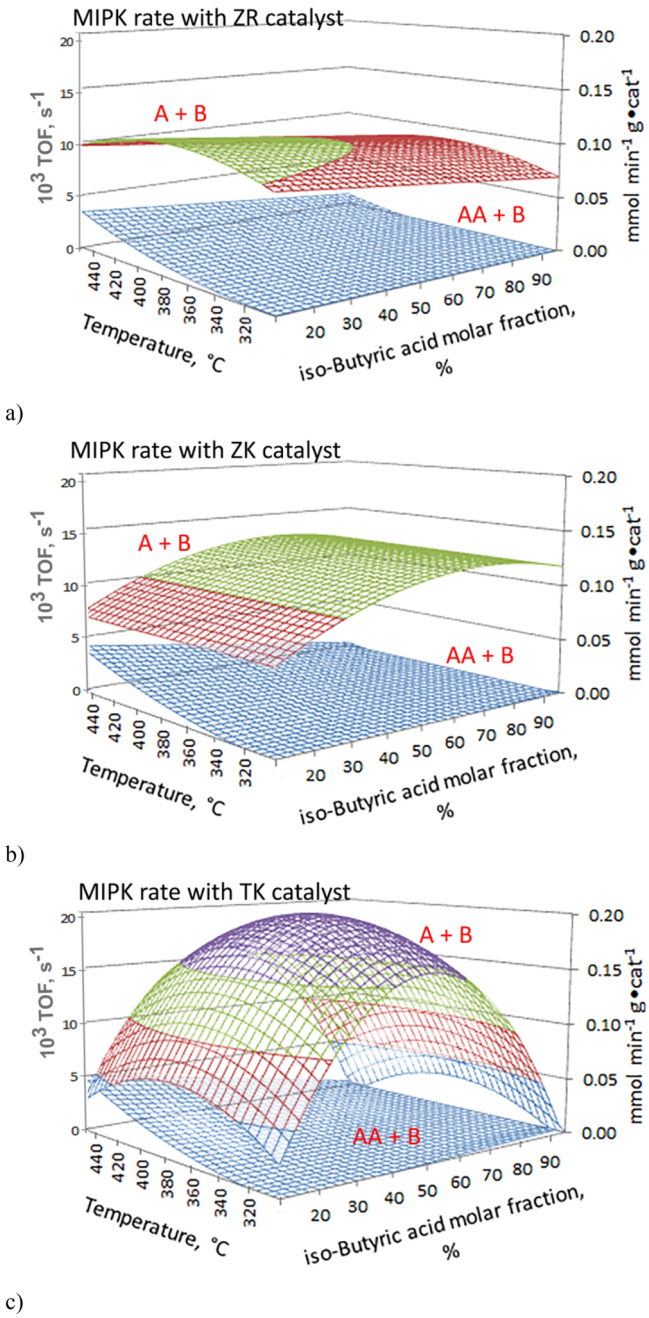

Figure 3. Comparison of MIPK (**AB**) rates of formation in the reaction of isobutyric acid (**B**) with acetone (**AA** + **B**) vs that with acetic acid (**A** + **B**) depending on temperature and molar fraction of isobutyric acid (**B**) at LHSV of 7 h^{-1} using (a) ZR, (b) ZK, and (c) TK catalysts.

deprotonation of the isopropyl group followed by condensation could lead to the symmetrical 1,3-diketone **ABA** formation (Scheme 4). Because of its symmetry, there is only one way to decompose **ABA,** that is, back to **AB** and **A**. If it does take place, condensation of MIPK (**AB**) with acetic acid (**A**) would be a degenerate reaction that remained unnoticed.

For the second direction, if the methyl group of MIPK is enolized, condensation could lead to the unsymmetrical 1,3-diketone **AAB**, which would decompose to a mixture of acetone (**AA**) and isobutyric acid (**B**) according to Scheme 5.

As shown in Section 3.1, the reaction in reverse to the equation in Scheme 5—acetone condensation with isobutyric acid—does take place. For this reason, even if the reaction **A** + **AB** does proceed leading either to **AAB** or to **AA** + **B**, more readily, it may go back to the mixture of **A** and **AB**. In such a case, condensation of the methyl side of MIPK with acetic acid will be unnoticed again. In addition, the reketonization of **AB**

Scheme 4. Possible AB Ketone Condensation with Acetic Acid A through Enolization on Isopropyl Group Side, a Degenerate Reaction

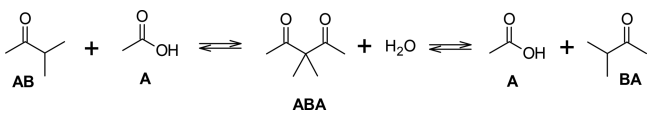

DOI: 10.1021/acsomega.9b01188
ACS Omega 2019, 4, 11032−11043

Scheme 5. Possible AB Ketone Condensation with Acetic Acid A through Enolization on Methyl Group Side

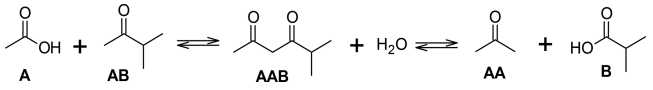

to **AA** is masked by a competing and much faster reaction—the regular condensation of acetic acid with itself followed by decarboxylative ketonization to acetone (Scheme 6).

Scheme 6. Decarboxylative Ketonization of Acetic Acid A

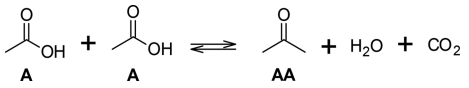

Similarly, in the attempted reketonization of DIPK (**BB**) with acetic acid (**A**), acetone was produced as the major product of acetic acid self-condensation (Scheme 7). Traces of MIPK (**AB**) and isobutyric acid (**B**) were detected only at high temperatures, 450 °C, and at a high concentration of DIPK.

Scheme 7. Attempted Reketonization of DIPK with Acetic Acid Provided Only Traces of AB and B

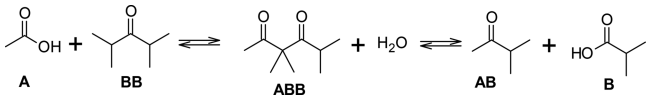

Reketonization was more successful for the reaction between isobutyric acid **B** and MEK (**CA**), which is only slightly less sterically hindered compared to MIPK. The reaction between **B** + **CA** proceeded in two directions from the entry point in the middle of Scheme 8.

Two products of the reketonization, **BC** and **AB**, along with the product of isobutyric acid self-condensation, **BB**, were obtained with the ZK catalyst (Figure S4). Identification of products was done by using GC/MS analysis and spiking with authentic samples. Reketonization of MEK with isobutyric acid was about tenfold slower compared to that with acetone (Figure 4). The relative amounts of **BC** versus **AB** were close to each other within the error of the experiment.

A common nature of the reketonization reaction was also confirmed by using a long-chain linear acid. A mixture of acetone and stearic (octadecanoic) acid in a 99:1 molar ratio was converted to nonadecan-2-one (Figure S5) at a temperature of 475 °C and LHSV of 2 h^{-1} with the ZK catalyst. Under those conditions, a full conversion of stearic acid was achieved. The calculated average rate of the reaction, 3.5 mkmol/min/g-cat, was lower than for isobutyric acid, but a direct comparison cannot be done in view of the full conversion. After all stearic acid had been consumed, products of acetone dimerization and trimerization started to form, such as mesityl oxide, isophorone, and 1,3,5-trimethylbenzene, typical for ketone condensation on metal oxides in the absence

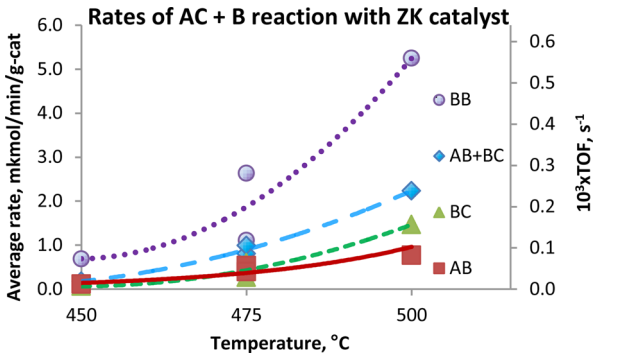

Figure 4. Average rates for the formation of products in the reketonization of methyl ethyl ketone **AC** with isobutyric acid: **BB**, **BC**, **AB**, and the combined rate of **AB** and **BC** at LHSV = 1 h^{-1} with ZK catalyst depending on temperature.

of carboxylic aicds.[25] MEK and MIPK also formed a similar type of product.

Activity of all catalysts has not declined below at least 90% of the initial value after approximately 80 h of testing time. Relative stability of the catalysts was found in the order TK > ZK > ZR, which was assessed by a small but measurable, less than 2%, weight increase at the end of the DOE set and also by a color change (Figure S6). There were no carbonaceous deposits formed on catalysts.

3.3. Condensation of Acetone with Isotopically Labeled Isobutyric Acid. Reketonization of acetone with isobutyric acid labeled on its carboxylic group by ^{13}C was studied with the ZK catalyst in the pulse microreactor inside GC/MS. The carbonyl group in the MIPK product was monitored by a mass spectrometry detector, and it was found to be composed of about 96% of ^{13}C. It was concluded based on the ratios of molecular ions m/z = 87 to m/z = 86 and isobutyryl ions m/z = 72 to m/z = 71. The fact that isobutyric acid being the exclusive source of the carbonyl group in MIPK is consistent with the reketonization mechanism outlined in Scheme 2.

The initial atomic percent of ^{13}C on the carboxyl group of isobutyric acid was 99%. The reason that it is decreased to 96% on the carbonyl group of the ketone product is most likely because of the $^{12}C/^{13}C$ exchange between labeled isobutyric acid and unlabeled CO_2, which we have recently described.[12] The unlabeled CO_2 may result from the secondary decarboxylative ketonization of acetic acid initially released in the reketonization of acetone.

3.4. Catalytic Decomposition of β-Diketones by the Retrocondensation Reaction. Because 1,3-diketones are proposed as the intermediates of the decarboxylative reketonization reaction in Scheme 2 yet are not isolated, they must decompose faster than they form. This assumption was verified in separate experiments by continuously feeding 1,3-diketone solutions in water or methanol to the hot tube reactor filled with a catalyst.

Decomposition of acetylacetone in water should initially produce acetone and acetic acid in an equal number of moles

Scheme 8. Successful Reketonization of CA Ketone with Isobutyric Acid B into Ketones BC and AB

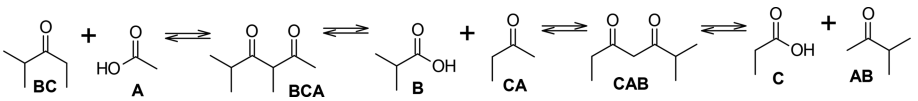

DOI: 10.1021/acsomega.9b01188
ACS Omega 2019, 4, 11032−11043

according to the reaction stoichiometry. However, the observed amounts of acetic acid and acetone in moles were not equal because part of acetic acid was immediately converted to acetone by the decarboxylative ketonization reaction according to Scheme 6. The rate of acetic acid conversion to acetone was calculated from the difference in apparent rates of acetone and acetic acid formation (Figure 5).

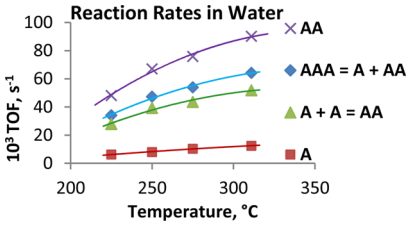

Figure 5. Decomposition rate of acetylacetone **AAA** 2.2% M solution in water, apparent rates of acetic acid **A** and acetone **AA** formation, and the calculated rate of acetic acid conversion into acetone **A** + **A** = **AA** with ZK catalyst at a residence time of 0.084 s.

To avoid complications due to the side reaction of acetic acid to acetone, decomposition of 1,3-diketones was studied in anhydrous methanol solution. In that case, methyl esters were formed instead of free acids together with ketones. Symmetrical 1,3-diketones, **AAA**, **ABA**, and **BAB**, produced only one pair of methyl ester and ketone, while unsymmetrical **AAB** ketone produced two pairs, **A** + **AB** and **AA** + **B** (Scheme 9).

Scheme 9. Retrocondensation of Unsymmetrical 1,3-Diketone AAB with Methanol into Two Pairs of Ester/Ketone

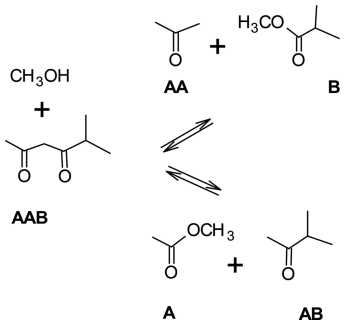

Because anhydrous methanol was used, methyl esters did not show any sign of hydrolysis, although some conversion to ketones could have occurred to a minor degree as evidenced by the slight asymmetry of the amount of ketones versus esters produced. Ketones were always produced in methanol in a slightly larger amount compared to esters (Table S4), but the difference was not as large as in water (Table S3 and Figure 5).

Decomposition of three symmetrical and one unsymmetrical 1,3-diketones in methanol was studied under pseudo-first-order reaction conditions with the same three catalysts using 1−3 mol % solutions at the temperature range of 200−400 °C. Initial data points (Table S4 in the Supporting Information) were used in a regression analysis to find coefficients for the rate dependence on concentration and temperature (Table S5). Reaction rates followed first-order dependence on the concentration of 1,3-diketone and quadratic polynomial dependence on the temperature (Figure S1).

The untreated zirconia catalyst (ZR) showed a significantly higher activity for the decomposition of 1,3-diketones in methanol compared to KOH-treated catalysts ZK and TK (Figure 6). With the ZR catalyst, the most reactive diketone

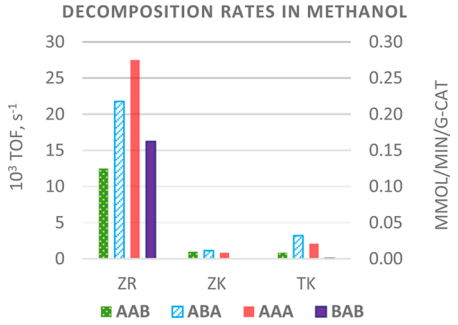

Figure 6. Decomposition rates of diketones 2% M solution in methanol with ZR, ZK, TK catalysts at the temperature of 300 °C and the residence time of 0.020 s (for compound abbreviations refer to Chart 1).

was the least substituted diketone **AAA**, acetylacetone, followed by **ABA**. With both KOH-treated catalysts, **ABA** becomes the most reactive diketone. Its high activity is explained in the Discussion section. Activity of all catalysts has not declined for the entire duration of the decomposition tests. Neither color change nor measurable weight gain has been detected at the end.

Decomposition of the unsymmetrical ketone **AAB** was faster in the direction of making ketone **AB** (MIPK) versus **AA** (acetone, Scheme 9). The preference for MIPK over acetone formation varies slightly with the temperature studied in the 250−350 °C range (Table S6) with the average being 70, 59, and 65% for ZR, ZK, and TK catalysts, respectively.

3.5. Adsorption of Ketones and Acids on Metal Oxides. The difference in the adsorption of ketones versus carboxylic acids was assessed by a pulse titration method using the "inside GC/MS microreactor". A small amount of a catalyst was placed inside the injection port of the GC/MS instrument, and premeasured pulses of organic molecules were added until a full saturation was achieved. The adsorbed amount for each pulse was calculated as the difference between amounts injected and coming out. Coverage was calculated by using the BET surface area and assuming a bidentate bridging mode of adsorption for carboxylic acids and a monodentate adsorption for ketones. For ketones, some bleeding from the surface was noticed only for the exposure time in flowing helium gas measured in hours. There were no significant differences between the calculated adsorptions of acetone when the time between pulses was set to 5, 10, and 30 min. Data obtained at the 10 min interval were reported in all experiments.

As can be seen in Figure 7, adsorption of carboxylic acids on the surface is much stronger compared to that of ketones. The difference between surface concentrations of carboxylic acids and ketones can be one of the reasons explaining the difference between the reaction rates of acetic acid versus acetone in their reaction with isobutyric acid making MIPK (Figure 3b).

3.6. DFT Modeling. The most important steps for the synthesis of diketones from carboxylic acids and ketones and for the decomposition of diketones in their reaction with water were modeled by DFT computations on the (111) surface of

DOI: 10.1021/acsomega.9b01188
ACS Omega 2019, 4, 11032−11043

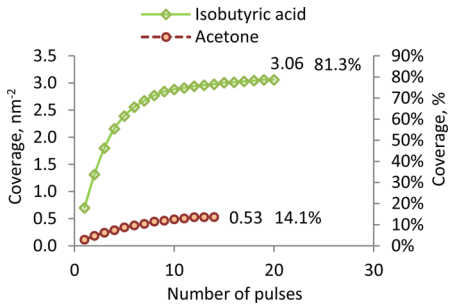

Figure 7. Adsorption of isobutyric acid and acetone measured in a pulse microreactor inside GC/MS at 200 °C by adding 0.1 μL pulses to 20 mg sample of ZK catalyst.

monoclinic zirconia using DMol^3 for periodic structures (Figures 8 and 9 and Table 1).

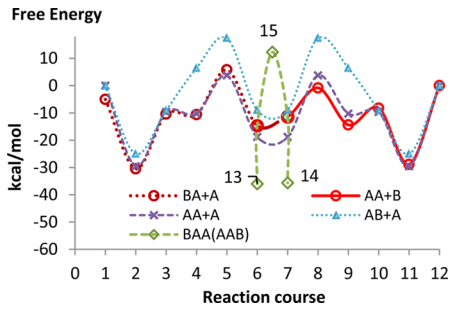

Figure 8. Free energy profile of the catalytic mechanism for three different reketonization reactions, **BA** + **A** = **AA** + **B** (Figure 9), **AA** + **A** = **A** + **AA** (Figure S2), **AB** + **A** = **A** + **BA** (Figure S3), following elementary steps of Scheme 10. Energies are shown relative to the energy of the empty surface and **AA** + **B** in the gas phase, structure **12**.

The size of the supercell was chosen to match experimentally determined concentration of acids on the zirconia surface, which is less than 3 nm^{-2} (Figure 7). The selected model accurately represents a high surface saturation, which seems to be an important factor in the decarboxylative ketonization mechanism.[11] Nonetheless, there were no close contacts shorter than 0.35 nm, and the model has been previously used to study a similar mechanism between two molecules of acids.[8]

We took advantage of the previous DFT study in which various options for the condensation step between two surface carboxylates have been already extensively studied. Accordingly, we have replaced the enolized carboxylate in the previous model with the enolized ketone.

Condensation between the enolized ketone in a monodentate adsorption mode and surface carboxylate in a bidentate bridging adsorption mode (structures **2** and **11**) is followed by dehydration of the resulting intermediate (structures **4** and **9**) and leads to diketones **6** and **7** (Figure 9a,b). Reverse steps in the opposite direction, that is, hydration of β-diketones **6** or **7** and C−C bond cleavage in structures **4** or **9** by retrocondensation (Figure 9b), lead to the complementary pair of the enolized ketone and carboxylic acid, **2** or **11**, according to Scheme 10.

Geometry was optimized, and frequency calculations were performed for all reactants, products, and transition states, as shown in Figure 9a,b and Figures S2 and S3. Thermodynamic quantities were computed from vibrational frequency calculations within the canonical transition state theory provided by the Materials Studio software package.

The free energy profile for the interconversion of structures **1**−**12** at 300 °C is shown in Figure 8. In the case of the unsymmetrical diketone, a universal graph is derived from a combination of red lines (**AA** + **B** and **A** + **AB**), which can be used to describe decomposition of the unsymmetrical β-diketone when entered from the middle of the catalytic cycle (structures **6** and **7**) or the interconversion between two pairs of acid/ketone represented by structures **1** or **12** according to Scheme 10. All energies are calculated relative to the empty surface with **AA** and **B** in the gas phase, **12**. Structure **1** represents an empty surface with **BA** and **A** in the gas phase, and it is 5.1 kcal/mol lower in energy compared to **12**. The energy of the gas phase **AAB** and the empty surface (structure **15**) is shown to characterize desorption of **AAB** from **6** and **7**. It is important to note that abstraction of the most acidic proton from surface diketones **6** and **7** proceeds with significant energy stabilization (21.3 and 24.2 kcal/mol) into structures **13** and **14**, respectively.

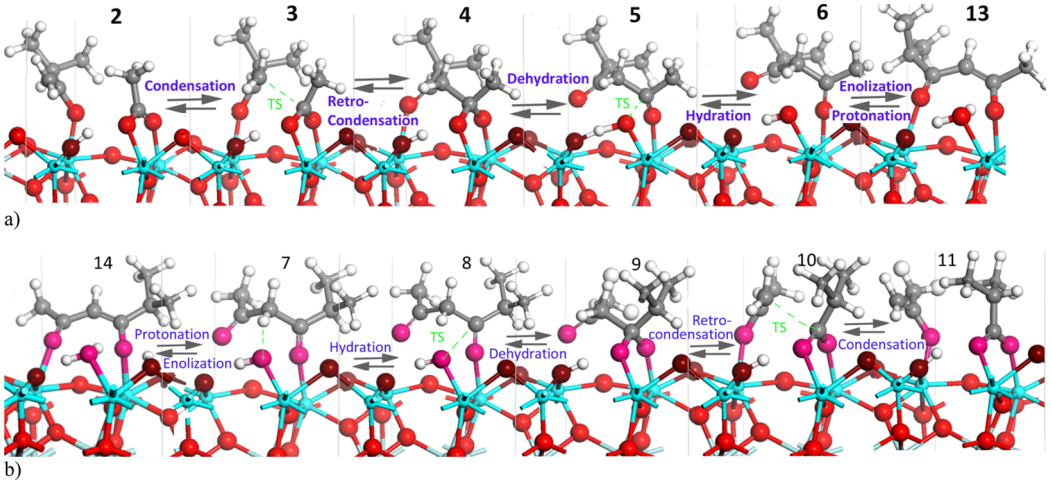

Figure 9. Elementary steps of the reaction mechanism on (111) surface of monoclinic zirconia for (a) **BA** + **A** = **BAA** reaction and (b) **BAA** = **B** + **AA** reaction according to Scheme 10.

DOI: 10.1021/acsomega.9b01188
ACS Omega 2019, 4, 11032−11043

Table 1. DFT-Calculated Free Energy of Activation and of Reaction (in Parenthesis), kcal/mol, for the Elementary Steps of the Reaction Mechanism on (111) Surface of Monoclinic Zirconia at 300 °C and the Equilibrium Fractions of Structures 2 and 11 Based on the Calculated Equilibrium Constant

ketone−acid pair, 1	fraction of 2 in the equilibrium between 2 and 11	condensation, 2 → 4	retrocondensation, 4 → 2	dehydration, 4 → 6	hydration, 6 → 4	enolization, 6 → 13	diketone, 6
BA + A	98.6%	20.1 (19.9)	0.2 (−19.9)	16.4 (−4.1)	20.5 (4.1)	–[a] (−21.3)	**BAA**
AA + A	50%	20.7 (20.2)	0.5 (−20.2)	13.9 (−10.6)	24.5 (10.6)	–[a] (−19.2)	**AAA**
AB + A	50%	16.0 (31.5)	−15.5 (−31.5)	11.0 (−15.4)	26.4 (15.4)		**ABA**
diketone, 7	enolization, 7 → 14	hydration, 7 → 9	dehydration, 9 → 7	retrocondensation, 9 → 11	condensation, 11 → 9	fraction of 11 in the equilibrium between 2 and 11	ketone acid pair, 12
AAB	–[a] (−24.2)	10.6 (−3.0)	13.5 (3.0)	6.1 (−14.5)	20.6 (14.5)	1.4%	**AA + B**
AAA	–[a] (−19.2)	24.5 (10.6)	13.9 (−10.6)	0.5 (−20.2)	20.7 (20.2)	50%	**A + AA**
ABA		26.4 (15.4)	11.0 (−15.4)	−15.5 (−31.5)	16.0 (31.5)	50%	**A + BA**

[a]En dash (−) indicates a barrierless process.

4. DISCUSSION

The data presented above show that methyl ketones, in general, and acetone, in particular, can condense with carboxylic acids in the vapor phase over metal oxide catalysts at temperatures above 300 °C. However, the immediate products of their condensation, β-diketones, are not stable under the reaction condition and decompose by the retrocondensation to a different pair of an acid and ketone. Formally, this reaction results in the transfer of the methyl group from acetone to the acyl group of the second carboxylic acid making methyl ketones.

Acetone itself is made from acetic acid under similar conditions by the decarboxylative ketonization reaction. Reusing acetone in the cross-ketonization with another acid makes it possible to prepare unsymmetrical ketones by the mechanism best described as reketonization. This reaction is of considerable importance for the industrial production of methyl ketones.[5] If not utilized, acetone would represent up to 50% loss of acetic acid together with a loss of the second carboxylic acid to the other symmetrical ketone, dramatically reducing cost-effectiveness of the cross-ketonization. On the other hand, reketonization of the desired cross-product, methyl ketone **AB**, is unwanted, but the main question is whether such a reaction does take place at all.

Experiments with isotopically labeled isobutyric acid (Section 3.3) showed that it is the exclusive source of the carbonyl group of MIPK and that we are dealing with an acid/base-catalyzed condensation of carbonyl compounds rather than with an alkyl group shift by some kind of concerted mechanism.

The unsymmetrical ketone **AB** has α-hydrogens on both sides of the carbonyl group, which allow its enolization and condensation with acids similar to that of acetone **AA**. If **AA** can condense with **B**, similarly, **AB** may condense with **A**.

Control of the forward reaction in Scheme 5 could be either of a thermodynamic or kinetic nature or a mixed one. If reactions in Scheme 5 are reversible in both directions and allowed to equilibrate, it might be shifted to the left, toward more stable mixture, **A** + **AB**. Indeed, thermodynamic quantities of the gas phase molecules obtained through vibrational frequency calculations by using the same DFT method as for periodic structures show that the mixture of **A** and **AB** is more stable compared to the mixture of **AA** and **B**. The DFT-calculated free energy difference in the gas phase at 300 °C is 5.07 kcal/mol, which relates to an equilibrium constant of 0.0118 and to the equilibrium fraction of **A** + **AB** equal to 98.8%. By itself, this is a sufficient reason for shifting the equilibrium in Scheme 5 to the left hand side, providing that the reaction conditions allow for the equilibrium to be established.

The same preference in favor of **A** + **AB** versus **AA** + **B** remains for structures on the surface (Figure 8). The DFT-calculated free energy for structure **2** representing **A** + **AB**, −30.5 kcal/mol, is 1.6 kcal/mol lower compared to that for structure **11** (**AA** + **B**), −28.9 kcal/mol (Table 1). However, decomposition of the unsymmetrical diketone **AAB** from the two possible adsorption states **6** and **7** (Figure 9a,b) has the lower calculated free energy barrier of the hydration step when going to the right hand side, that is, toward **AA** + **B**. Condensation steps are not a differentiating factor because the free energy barriers for both directions of the condensation, **AA** + **B** or **A** + **AB**, are almost the same, 20.6 kcal/mol or 20.1

DOI: 10.1021/acsomega.9b01188
ACS Omega 2019, 4, 11032−11043

Scheme 10. Mechanism of the Catalytic Reketonization Reaction between Mixture of AA + B and BA + A via Formation of Unsymmetrical 1,3-Diketone AAB (the Same as BAA) on Surface of ZrO_2

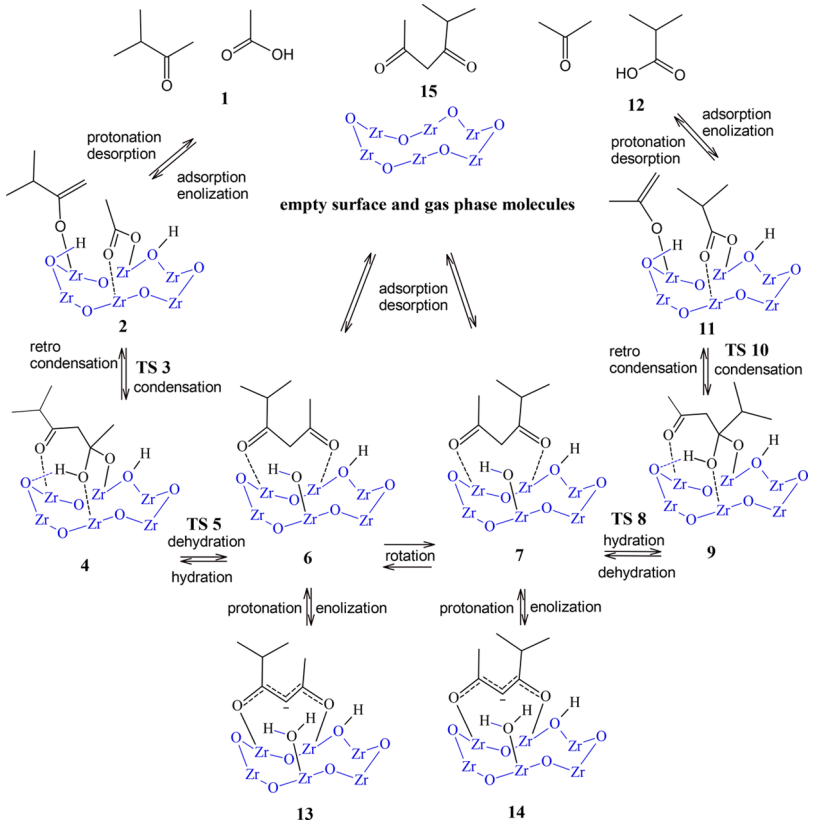

kcal/mol, respectively (Table 1). Therefore, DFT computations predict **AA** + **B** to be the major direction for β-diketones decomposition under kinetic control, while **A** + **AB** will be favored under thermodynamic control.

Experimentally, we have found only a small but persistent preference for the direction of the unsymmetrical diketone **AAB** decomposition in methanol toward **A** + **AB** rather than the **AA** + **B** mixture in Scheme 4. The preference for the formation of a more substituted ketone is about 70% with ZR or 60% with the ZK catalyst (Table S6), that is, not as large as the 98.8% value expected under purely thermodynamic control. The use of methanol as a nucleophile instead of water was necessary to reveal the selectivity of the initial decomposition by the retrocondensation reaction while avoiding further reactions between acids such as **A** + **A** = **AA**, which takes place in water (Figure 5). Methyl esters formed in methanol are generally much less reactive in the decarboxylative ketonization reaction compared to acids.[26]

Thus, experimental results indicate that β-diketone decomposition is controlled kinetically, but the initial ratio of products changes to some extent by the reverse reaction toward the thermodynamic equilibrium. From the energy profile shown in Figure 8, it can be seen that both desorption steps, **2** → **1** and **11** → **12**, have high energy barriers. Hence, surface species **2**–**11** located in the energy well become involved in a thermodynamic equilibrium between important steps of the reketonization mechanism, C–C bond breaking and formation.

However, the most important factor controlling the direction of the reketonization equilibrium seems to be a higher reactivity of acetic versus isobutyric acid in the decarboxylative self-ketonization reaction,[4] and both acids have much higher rates in the decarboxylative ketonization relative to the reketonization reaction (directly compared in Figures 2 and 3). A faster consumption of acetic acid versus isobutyric leads to its selective removal from the equilibrium in Scheme 5, shifting it to the left hand side. In addition, a self-condensation of the released acetic acid back to acetone generates more feed for the reketonization of acetone and isobutyric acid into MIPK, **AB**, so the overall process at its limit is described by Scheme 11.

Scheme 11. Balanced Equation for the Reketonization of Acetone into MIPK with Isobutyric Acid

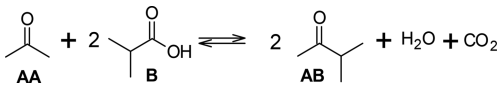

The calculated equilibrium constant for the reaction in Scheme 11 at the temperature 300 °C is 4.9×10^7 leading to the equilibrium concentration of **AA** + **B** less than 2.0×10^{-6}%, which explains reketonization of acetone **AA** into MIPK **AB**.

In a similar fashion, the reaction between ketone **AC** and acid **B**, going to the edges from the middle of the equation in Scheme 8, is able to proceed because it releases two acids, **A** and **C**, both of which are consumed faster on metal oxide surfaces compared to acid **B** and are removed from the equilibrium. It is due to the well-known fact that less sterically hindered acids are more reactive in the decarboxylative ketonization.

DOI: 10.1021/acsomega.9b01188
ACS Omega 2019, 4, 11032–11043

Interestingly, ketone **AC** (2-butanone) was believed to be inert and used as a solvent for that reason in a number of decarboxylative ketonization studies, for example, in a mixture with butyric, pentanoic, and hexanoic acids using a ceria–zirconia catalyst.[26] However, the temperature in those studies did not exceed 350 °C, and products of reketonization were not noticed.

We may now conclude that the reaction between **A** and **AB** in Schemes 4 and 5, most likely, does take place, but it is masked and hard to detect. The exact kinetic consequence of all reketonization reactions has yet to be determined. It is clear that a number of side reactions may inhibit the rate of the decarboxylative ketonization of carboxylic acids. Conceivably, the major contributor to such inhibition is the degenerate reaction in Scheme 12 between acetone and acetic acid, a pair of the least substituted and sterically less hindered ketone and acid.

Scheme 12. Degenerate Reaction between Acetone and Acetic Acid

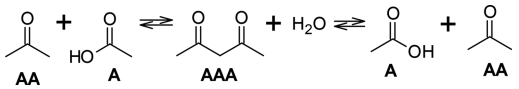

As the conversion of acids is increasing and more ketones are produced, a larger portion of catalytic sites becomes occupied with the reketonization reaction slowing down the overall rate of ketone production. The reason for the inhibition of the rate of decarboxylative ketonization of acetic acid by the acetone product was previously thought to be its accumulation on the surface.[27,28] However, acetone adsorption on the surface is much weaker compared to that of acids (Figure 7). A comparable amount of acetic and isobutyric acids adsorbed on zirconia at the temperature range of 200–400 °C was found previously.[4,19] Therefore, the most likely reason for the above inhibition is the reketonization reaction according to Scheme 12, which is more prevalent compared to the recently reported condensation between acetone and carbon dioxide.[12]

The apparent rate of MIPK formation was found to be lower when starting from acetone versus acetic acid in the reaction with isobutyric acid (Figure 3a–b). Because the ratio of surface concentrations of ketones to acids is approximately equal to the ratio of their apparent rates in the reaction with isobutyric acid (Figure 7), we may conclude that the rate constants of the rate limiting step, condensation, in the decarboxylative ketonization versus reketonization reaction are of a comparable order of magnitude.

The heterogeneous version of the retrocondensation reaction of diketones catalyzed by zirconium and titanium metal oxides in our study is closely related to the two mechanisms of β-diketones and β-keto esters decomposition known in the literature. The first one is the retrocondensation through a preliminary chelate complexation in the solution by many other transition metals, such as Co, Zn, Cu, Ni, Pd, Mn, Pt, and Rh.[29] The second one is a direct attack by strong nucleophiles such as NaOH and $NaOC_2H_5$, both in the solution and in the solid state.[30] Zirconium and titanium oxides in our study can provide conditions for both types of the retrocondensation mechanism through complexation of dicarbonyls on the surface and by hosting water and methanol nucleophiles (Figure 9a,b). In that regard, the untreated zirconia catalyst, ZR, showed higher activity for retrocondensation because of its known ability to hold more of dissociatively adsorbed water on the surface compared to KOH-treated catalysts,[18] and a similar difference can be expected for methanol adsorption. Both nucleophiles, hydroxy and methoxy groups, play a critical role in the decomposition of diketones by attacking a carbonyl group of β-diketones.

An important factor, which may slow down the retrocondensation step, is the enolization of β-diketones proceeding with a large energy of stabilization according to the DFT calculations. The position of the enolized diketone structures **13** and **14** on the energy diagram is the lowest among all intermediates on the surface (Figure 8). Quantitative enolization of the condensation product in the classic Claisen reaction in solutions is an essential step, which makes that reaction possible.[31] Likewise, due to a high C–H acidity, enolizable β-diketones are taken out of the condensation equilibrium by reacting with basic centers on the catalyst surface, which helps to advance the condensation step forward. In contrast, non-enolizable β-diketones with alkylated methylene groups, such as diketone **ABA**, are difficult to synthesize using nucleophilic bases because the equilibrium of the Claisen condensation may shift back as the result of the nucleophilic attack by such bases on the keto form.[32] It was the reason, for which we had to use a non-nucleophilic base, NaH, for the preparation of **AAB** in our work to increase its yield (Section 2.4).[33] Because a higher activity was found for the non-enolizable diketone **ABA** relative to enolizable diketones in the retrocondensation reaction with all catalysts (Figure 6), enolization of diketones and β-keto carboxylates may take place and be an important part of the catalytic decarboxylative ketonization mechanism and for all concomitant steps discussed in our study.

5. CONCLUSIONS

Decarboxylative cross-ketonization of carboxylic acids is surrounded by rich chemistry driven by a sequence of condensation and retrocondensation steps including decarboxylation. We have disclosed additional side reactions in the decarboxylative ketonization mechanism in which not only carboxylic acids but also ketones can enolize on the surface of metal oxides and participate in the condensation reactions as nucleophiles. Their electrophilic partners for condensations are surface carboxylates and carbon dioxide molecules. Only in the absence of carboxylic acids and carbon dioxide, ketones are able to go through a usual aldol condensation with another ketone molecule.

All reactions are reversible and affected to a various degree by the thermodynamic stability of products. The equilibrium in the catalytic condensation between ketones and carboxylic acids leading to β-diketone intermediates is shifted away from the β-diketones. In the case of unsymmetrical diketones, the preferred direction of their decomposition is toward formation of a more reactive carboxylic acid due to its faster disappearance in the decarboxylative homoketonization. The reketonization effect is observed in the reaction between a less reactive acid and a ketone derived from a more reactive acid, typically, acetone.

A catalyst activity in such chemistry depends on its acid–base properties and the surface structure. Because there are no redox steps involved in the reaction mechanism, possession of a redox function by metal oxide catalysts is unnecessary for the decarboxylative ketonization and for the reketonization reactions.

DOI: 10.1021/acsomega.9b01188
ACS Omega 2019, 4, 11032–11043

■ ASSOCIATED CONTENT

Supporting Information

The Supporting Information is available free of charge on the ACS Publications website at DOI: 10.1021/acsomega.9b01188.

Regression analysis for the rates of isobutyric acid condensation with acetone, decomposition of 1,3-diketones in water and methanol, and figures for **AA** + **A** = **AAA** and **AB** + **A** = **ABA** DFT calculations of elementary steps (PDF)

■ AUTHOR INFORMATION

Corresponding Author

*E-mail: alexey.ignatchenko@gmail.com. Phone: (585) 385-8385.

ORCID

Alexey V. Ignatchenko: 0000-0002-7806-6857

Notes

The authors declare no competing financial interest.

■ ACKNOWLEDGMENTS

T.J.D., H.P., and J.R.L. are grateful for the support by the Summer Science Research Programs at St. John Fisher College in 2014 and 2015. We thank Dr. Evguenii Kozliak (University of North Dakota) for useful comments and former SJFC undergraduate students Laura Moore and Roberto M. Voica for their participation at the beginning of this project.

■ REFERENCES

(1) Ignatchenko, A. V.; King, M. M.; Liu, Z.; Whiddon, C. W. Catalysts Selective for the Preparation of Mixed Ketones from a Mixture of Carboxylic Acids. U.S. Patent 7,659,432, 2010.

(2) Ignatchenko, A. V.; King, M. M. Catalyst for the Production of Methyl Isopropyl Ketone. U.S. Patent 7,501,379, 2009.

(3) Ignatchenko, A. V.; King, M. M.; Liu, Z.; Whiddon, C. W. Catalysts Selective for the Preparation of Mixed Ketones from a Mixture of Carboxylic Acids. U.S. Patent 7,452,841, 2008.

(4) Ignatchenko, A. V.; DeRaddo, J. S.; Marino, V. J.; Mercado, A. Cross-Selectivity in the Catalytic Ketonization of Carboxylic Acids. *Appl. Catal., A* **2015**, *498*, 10−24.

(5) Schommer, C.; Ebel, K.; Dockner, T.; Irgang, M.; Hoelderich, W. Harald Rust. Preparation of Ketones. U.S. Patent 4,950,763, 1990.

(6) Gorman, M. The History of Acetone, 1600-1850. *Chymia* **1962**, *8*, 97−104.

(7) Kumar, R.; Enjamuri, N.; Shah, S.; Al-Fatesh, A. S.; Bravo-Suárez, J. J.; Chowdhury, B. Ketonization of Oxygenated Hydrocarbons on Metal Oxide Based Catalysts. *Catal. Today* **2018**, *302*, 16−49.

(8) Ignatchenko, A. V.; McSally, J. P.; Bishop, M. D.; Zweigle, J. Ab Initio Study of the Mechanism of Carboxylic Acids Cross-Ketonization on Monoclinic Zirconia via Condensation to Beta-Keto Acids Followed by Decarboxylation. *Mol. Catal.* **2017**, *441*, 35−62.

(9) Pham, T. N.; Sooknoi, T.; Crossley, S. P.; Resasco, D. E. Ketonization of Carboxylic Acids: Mechanisms, Catalysts, and Implications for Biomass Conversion. *ACS Catal.* **2013**, *3*, 2456.

(10) Pacchioni, G. Ketonization of Carboxylic Acids in Biomass Conversion over TiO_2 and ZrO_2 Surfaces: A DFT Perspective. *ACS Catal.* **2014**, *4*, 2874−2888.

(11) Wang, S.; Iglesia, E. Experimental and Theoretical Assessment of the Mechanism and Site Requirements for Ketonization of Carboxylic Acids on Oxides. *J. Catal.* **2017**, *345*, 183−206.

(12) Ignatchenko, A. V.; Cohen, A. J. Reversibility of the Catalytic Ketonization of Carboxylic Acids and of Beta-Keto Acids Decarboxylation. *Catal. Commun.* **2018**, *111*, 104−107.

(13) DiProspero, T. J.; Patel, H.; Ignatchenko, A. V. Catalytic Condensation of Ketones with Carboxylic Acids. In *24th North American Catalysis Society Meeting*; St. John Fisher College: Pittsburgh, PA, 2015; Vol. *11885*.

(14) Yang, D.; Zhou, Y.; Xue, N.; Qu, J. Synthesis of Trifluoromethyl Ketones via Tandem Claisen Condensation and Retro-Claisen C-C Bond-Cleavage Reaction. *J. Org. Chem.* **2013**, *78*, 4171−4176.

(15) Barkley, L. B.; Levine, R. The Synthesis of Certain Ketones and α-Substituted β-Diketones Containing Perfluoroalkyl Groups. *J. Am. Chem. Soc.* **1953**, *75*, 2059−2063.

(16) Harada, R.; Shigetomi, T.; Miyazaki, S.; Saito, M. Method for Extracting Asymmetric Beta-Diketone Compound from Beta-Diketone Compound. WO application 2014069240, 2014.

(17) Perfett, B. M.; Levine, R. A Study of Acid Catalysis in Ketone Acylations. *J. Am. Chem. Soc.* **1953**, *75*, 626−628.

(18) Ignatchenko, A.; Nealon, D. G.; Dushane, R.; Humphries, K. Interaction of Water with Titania and Zirconia Surfaces. *J. Mol. Catal. A: Chem.* **2006**, *256*, 57−74.

(19) Ignatchenko, A. V.; Kozliak, E. I. Distinguishing Enolic and Carbonyl Components in the Mechanism of Carboxylic Acid Ketonization on Monoclinic Zirconia. *ACS Catal.* **2012**, *2*, 1555−1562.

(20) Delley, B. From Molecules to Solids with the $DMol^3$ Approach. *J. Chem. Phys.* **2000**, *113*, 7756−7764.

(21) Ignatchenko, A. V. Density Functional Theory Study of Carboxylic Acids Adsorption and Enolization on Monoclinic Zirconia Surfaces. *J. Phys. Chem. C* **2011**, *115*, 16012−16018.

(22) Perdew, J. P.; Burke, K.; Ernzerhof, M. Generalized Gradient Approximation Made Simple. *Phys. Rev. Lett.* **1996**, *77*, 3865−3868.

(23) Tkatchenko, A.; Scheffler, M. Accurate Molecular Van Der Waals Interactions from Ground-State Electron Density and Free-Atom Reference Data. *Phys. Rev. Lett.* **2009**, *102*, No. 073005.

(24) Govind, N.; Petersen, M.; Fitzgerald, G.; King-Smith, D.; Andzelm, J. A Generalized Synchronous Transit Method for Transition State Location. *Comput. Mater. Sci.* **2003**, *28*, 250−258.

(25) Luo, S.; Falconer, J. L. Acetone and Acetaldehyde Oligomerization on TiO_2 Surfaces. *J. Catal.* **1999**, *185*, 393−407.

(26) Gaertner, C. A.; Serrano-Ruiz, J. C.; Braden, D. J.; Dumesic, J. A. Ketonization Reactions of Carboxylic Acids and Esters over Ceria-Zirconia as Biomass-Upgrading Processes. *Ind. Eng. Chem. Res.* **2010**, *49*, 6027−6033.

(27) Rajadurai, S. Pathways for Carboxylic Acid Decomposition on Transition Metal Oxides. *Catal. Rev.* **2006**, *36*, 385−403.

(28) Kuriacose, J. C.; Jungers, J. C. The Kinetics of the Decarboxylation of Fatty Acids on Thorium Oxide. *Bull. des Soc. Chim. Belges* **1955**, *64*, 502−534.

(29) Akhrem, I. S.; Vartanyan, R. S.; Afanas'eva, L. V.; Vol'pin, M. E. Splitting of C-C Bonds in β-Dicarbonyl Compounds Catalyzed by Transition Metal Complexes. *Bull. Acad. Sci. USSR, Div. Chem. Sci.* **1983**, *32*, 1217−1220.

(30) Smith, M. B.; March, J. Basic Cleavage of Beta-Keto Esters and Beta-Diketones. In *March's Advanced Organic Chemistry*; John Wiley & Sons, Inc.: 2001; pp 812−813.

(31) Wade, L. G. *Organic Chemistry*; 8th ed.; Pearson: Boston, 2013.

(32) Hauser, C. R.; Renfrow, W. B., Jr. Certain Condensations Brought about by Bases. I. The Condensation of Ethyl Isobutyrate to Ethyl Isobutyryl-isobutyrate1. *J. Am. Chem. Soc.* **1937**, *59*, 1823−1826.

(33) Swamer, F. W.; Hauser, C. R. Claisen Acylations and Carbethoxylations of Ketones and Esters by Means of Sodium Hydride[1]. *J. Am. Chem. Soc.* **1950**, *72*, 1352−1356.

DOI: 10.1021/acsomega.9b01188
ACS Omega 2019, 4, 11032−11043